ARTICLES
PUBLISHED ONLINE: 11 JULY 2016 | DOI: 10.1038/NCLIMATE3082
nature climate change

Multi-year persistence of the 2014/15 North Pacific marine heatwave

Emanuele Di Lorenzo[1]* and Nathan Mantua[2]

Between the winters of 2013/14 and 2014/15 during the strong North American drought, the northeast Pacific experienced the largest marine heatwave ever recorded. Here we combine observations with an ensemble of climate model simulations to show that teleconnections between the North Pacific and the weak 2014/2015 El Niño linked the atmospheric forcing patterns of this event. These teleconnection dynamics from the extratropics to the tropics during winter 2013/14, and then back to the extratropics during winter 2014/15, are a key source of multi-year persistence of the North Pacific atmosphere. The corresponding ocean anomalies map onto known patterns of North Pacific decadal variability, specifically the North Pacific Gyre Oscillation (NPGO) in 2014 and the Pacific Decadal Oscillation (PDO) in 2015. A large ensemble of climate model simulations predicts that the winter variance of the NPGO- and PDO-like patterns increases under greenhouse forcing, consistent with other studies suggesting an increase in the atmospheric extremes that lead to drought over North America.

During the fall of 2013 a large warm temperature anomaly developed in the upper ocean along the axis of the North Pacific Current. As the anomaly spread over a broad region of the Gulf of Alaska (GOA) during the winter of 2013/14, it reached a record-breaking amplitude with sea surface temperature anomalies (SSTa) exceeding three standard deviations (∼3 °C) (Fig. 1a and Supplementary Fig. 1, see Methods for a description of the datasets and definition of the SSTa indices). The onset and growth of this unusual water mass anomaly is attributed to forcing associated with a persistent atmospheric ridge over the northeast Pacific[1] (Fig. 1b) that is connected to the North Pacific Oscillation (NPO), a leading pattern of atmospheric variability[2]. Extreme amplitude and persistence in the NPO pattern is also implicated in the record drought conditions that affected California in the winter of 2013/14[3–5] and its expression is a known precursor of El Niño conditions[6,7]. By the summer and fall of 2014, the warm anomalies reached the Pacific coastal boundary of North America, and although the amplitude in the GOA and the northern California Current System (CCS) were reduced, record-high SSTa were found in the regions of southern and Baja California (Fig. 1c). In the winter of 2014/15, the SSTa over the entire northeast Pacific re-intensified, exceeding again the 3 °C threshold (Fig. 1e and Supplementary Fig. 1). The record-breaking high-temperature and the multi-year persistence of this warm anomaly, here referred to as a marine heatwave[8], have had unprecedented impacts on multiple trophic levels of the marine ecosystem and socio-economically important fisheries. Associated ecosystem impacts included low primary productivity[9], 11 new warm-water copepod species to the northern California Current shelf/slope region[10], a massive influx of dead or starving Cassin's auklets (sea birds) onto Pacific Northwest beaches from October through December 2014[11], a large whale unusual mortality event in the western GOA in 2015[12], and a California sea lion unusual mortality event in California from 2013–2015[13]. Severe, negative socio-economic impacts resulted from the 2015 harmful algal bloom that extended from southern California to southeast Alaska, the largest ever recorded[14]. Toxins produced by the extreme harmful algal bloom contaminated shellfish in Washington, Oregon and California, prompting prolonged closures for valuable shellfish fisheries. Although the socio-economic consequences of this climate event need to be further evaluated, it is possible that the northeast Pacific warm anomaly of 2014–15 is the most ecologically and economically significant marine heatwave on record.

Although previous studies[1,3,15–17] have documented the onset and nature of the atmospheric variability that forced the winter 2013/14 SSTa, the dynamics underlying the persistence and re-intensification of the anomaly in 2015 are still unclear. The relative role of ocean internal dynamics versus direct atmospheric forcing in driving the expression of the 2015 SSTa has not been examined. It is also unclear if the January–February–March (JFM) 2014 and JFM 2015 SSTa patterns (Fig. 1a and e) are dynamically linked, and if they are, how? There is good evidence that atmospheric teleconnections of tropical origin played a key role in the winter 2013/14 sea-level pressure anomalies (SLPa)[4,15–17] (Fig. 1b), and that the variance of this anomaly pattern may intensify under greenhouse forcing[3,4], hence leading to more extremes in ocean temperature and western US precipitation. This raises the question of whether tropical/extratropical teleconnections were also important in driving the exceptional SSTa in the winter of 2014/15.

Atmospheric forcing of the marine heatwave

To understand the role of atmospheric forcing in driving the strong North Pacific warm anomalies, we begin by inspecting maps of the seasonal evolution of SSTa and SLPa between JFM 2014 and JFM 2015 (Fig. 1). The patterns of the peak SSTa in JFM 2014 and 2015 show important spatial differences. Whereas in 2014 the core SSTa are centred in the GOA (Fig. 1a) and exhibit a NPGO-like expression[18] or Victoria Pattern[19], in 2015 the largest warm anomalies are further to the east and extend along the entire Pacific North American coastal boundary, resembling the expression of the PDO[20], also referred to as the 'ARC' pattern (Fig. 1e). These differences in SSTa patterns are mirrored by a change in the SLPa patterns, which exhibit a strong dipole system in JFM 2014, typical of the NPO[2] (Fig. 1b), and a more pronounced single SLPa low in 2015, resembling the expression of a deeper and southeastward extended Aleutian Low (Fig. 1f). To measure the strength of the 2014 and 2015 anomaly patterns we compute the average SSTa in

[1]School of Earth and Atmospheric Sciences, Georgia Institute of Technology, Atlanta, Georgia 30332, USA. [2]Southwest Fisheries Science Center, National Marine Fisheries Service, National Oceanographic and Atmospheric Administration, 110 Shaffer Road, Santa Cruz, California 95060, USA.
*e-mail: edl@gatech.edu

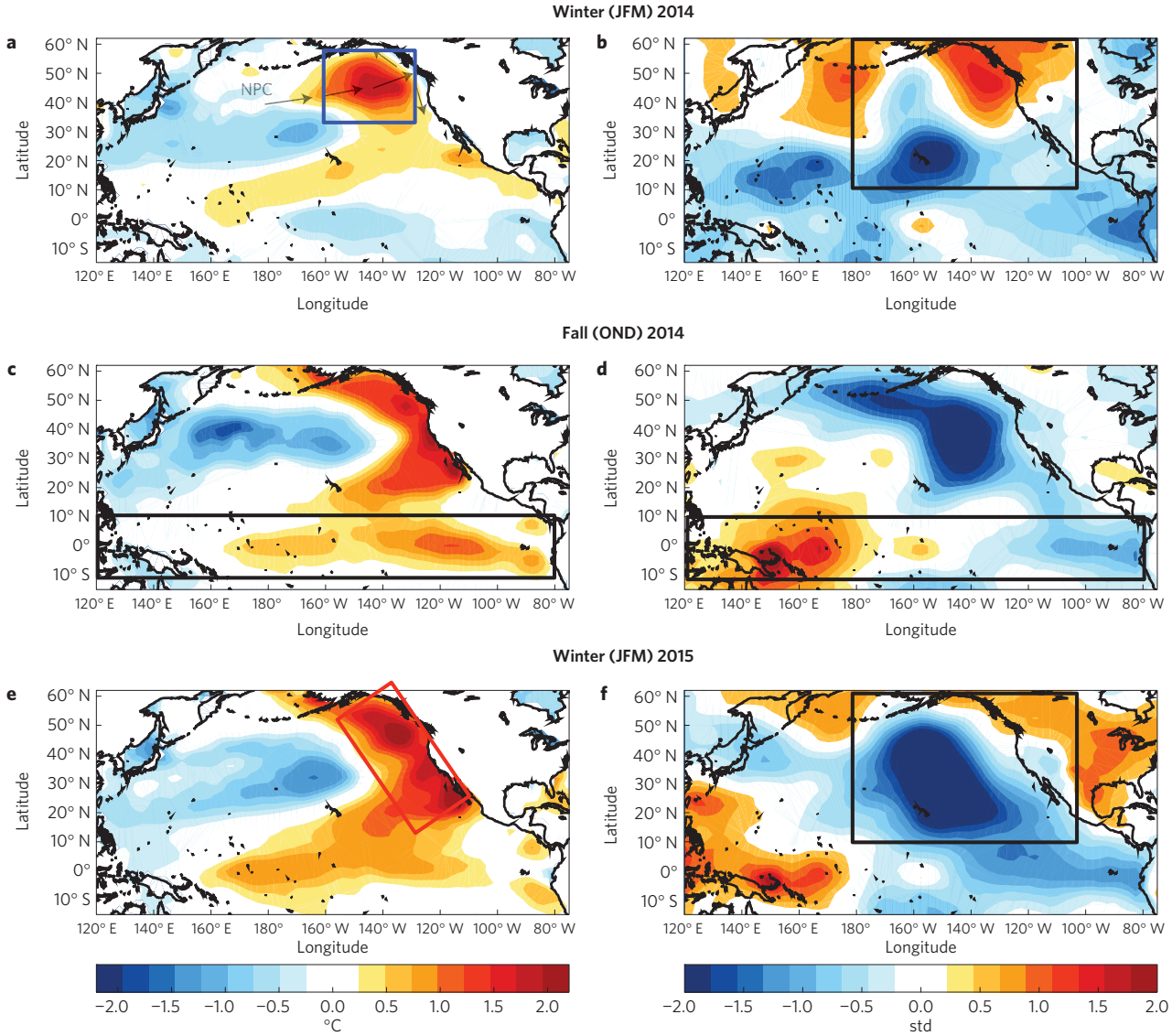

Figure 1 | Evolution of seasonal NOAA SSTa and NCEP SLPa during 2014 and 2015. a,**b**, January–February–March (JFM) 2014 SSTa and SLPa, respectively. **c**,**d**, October–November–December (OND) 2014 SSTa and SLPa, respectively. **e**,**f**, JFM 2015 SSTa and SLPa, respectively. The blue box in **a** denotes region used to compute the GOA SSTa index. The red box in **e** denotes region used to compute the ARC SSTa index. The mean position and direction of the North Pacific Current (NPC) and gyre circulation in the North Pacific Ocean is indicated with the grey arrows in panel **a**. Std: units of standard deviation.

the regions centred around the peak anomalies (Fig. 1a, blue box for 2014 pattern; Fig. 1e, red box for the 2015 pattern). We refer to these indices as the GOA SSTa index (shown in Fig. 2c) and the ARC SSTa index (shown Fig. 2d). With these definitions, the GOA and ARC SSTa indices (Fig. 2c,d) clearly capture the 2014 and 2015 anomalies as the largest SSTa ever recorded (>3 °C) (see also Supplementary Fig. 1), and reveal that the peak anomalies shifted from the central GOA in 2014 to the coastal GOA and CCS in 2015. The winter (JFM) variability captured by these targeted indices is identical to the first two principal components of JFM SSTa in the northeast Pacific, with correlations of $R > 0.9$ (Supplementary Fig. 2, see Methods), and is consistent with the JFM NPGO and PDO variability, with correlations of $R > 0.7$ (Supplementary Fig. 2).

To quantify to what extent the SSTa in 2014 and 2015 are forced by changes in the atmosphere, we derive temporal indices for the SLPa forcing patterns that were active during the 2014 and 2015 events; we refer to these as SLPa GOA and ARC indices (Fig. 2a,b) (see Methods for indices definitions). Inspection of the cross-correlation function between the SLPa and SSTa indices shows a maximum correlation when the SLPa are leading the SSTa by one to three months (see Supplementary Fig. 3), confirming that in the northeast Pacific the large-scale ocean SSTa are being forced by the atmosphere[21,22]. This forcing and response relationship is tested by reconstructing the GOA and ARC SSTa indices using a simple one-dimensional (1D) auto-regressive model (AR-1) forced by the corresponding SLPa indices (see Methods). A comparison of the observed and the AR-1 reconstructed SSTa indices (Fig. 2e,f) reveals high skill in capturing the strong peaks of 2014 for the GOA index (Fig. 2e) and of 2015 for the ARC index (Fig. 2f). The AR-1 model also exhibits skill in capturing the long-term variability of the GOA SSTa index ($R = 0.72$) and ARC SSTa index ($R = 0.83$), demonstrating that these ocean and atmospheric patterns of variability are recurrent in this region (for example, NPGO-like and PDO-like).

Multi-year persistence of warm anomalies

We have shown that both the 2014 and 2015 SSTa patterns can be reconstructed independently using direct atmospheric forcing functions. This suggests that ocean internal processes may not have

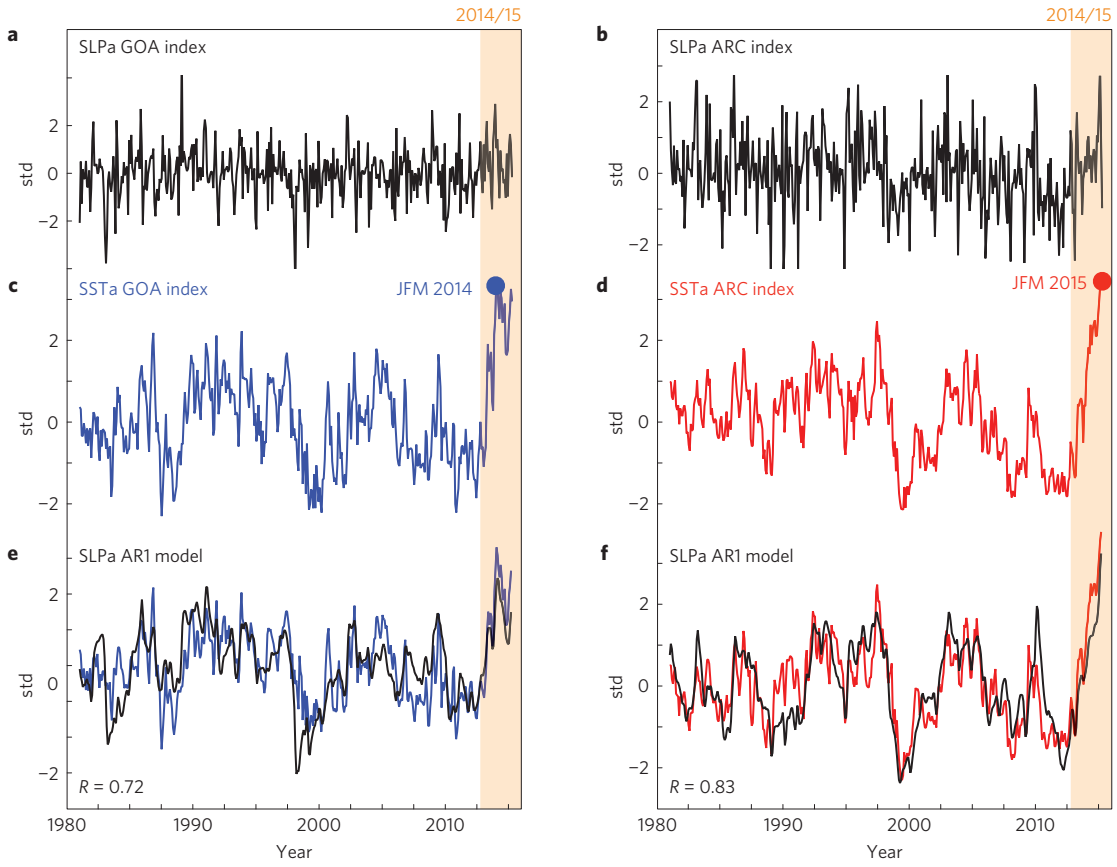

Figure 2 | Temporal variability of GOA and ARC patterns. a,**b**, Indices of the SLPa forcing derived from the GOA 2014 (**a**) and ARC 2015 (**b**) forcing patterns anomalies (see Fig. 1 panels **b** and **f**). **c**,**d**, Indices measuring the SSTa pattern for JFM 2014 (**c**, GOA SSTa index) and JFM 2015 (**d**, ARC SSTa index). **e**,**f**, Reconstructions of the GOA (**e**) and ARC (**f**) SSTa indices using an auto-regressive model forced by the SLPa GOA index (**a**) and the SLPa ARC index (**b**) time series, respectively. The correlation skill is significant above the 99% level. Std: units of standard deviation.

played a key role in persisting and evolving the record amplitude of the SSTa through 2015. For example, the mean ocean gyre advection of the 2014 anomaly (Fig. 1a) from the central GOA towards the North American coastal region may not have been important in shaping the expression of the 2015 SSTa (Fig. 1e). This raises an important question of whether the multi-year persistence of the SSTa expressions of 2014 and 2015 are dynamically linked, or if they occurred independently by random chance.

To establish the statistical relationship between the SSTa expressions of JFM 2014 and JFM 2015, we examine the temporal and spatial cross-correlation between the GOA and ARC SSTa indices (Fig. 3). The cross-correlation function is computed for the 1980–2012 data to exclude the strong 2014/15 event. At lag 0 month (Fig. 3a), the two indices share significant correlation ($R = 0.7$) because the areas used to define the GOA and ARC indices overlap in the Alaskan gyre region. As we inspect the lead/lag relationships at 1 year (for example, 12 months lead/lag in Fig. 3a) we find that the cross-correlation function is not symmetric, but instead shows a lobe with significant correlation ($R = 0.4$) when the GOA pattern leads the ARC pattern (right hand side of Fig. 3a). In contrast, the ARC pattern never leads significantly the GOA pattern. Inspection of the spatial structure of the SSTa leading to the ARC pattern (Fig. 3b–d) reveals the emergence of an El Niño expression (6 months lead) in the tropics during the progression from the GOA (12 month lead) to the ARC pattern. Consistent with this lead/lag relationship, a composite analysis of JFM SSTa events reveals that the ARC SSTa pattern typically emerges after a strong GOA SSTa event (Supplementary Fig. 1). Strong consecutive multi-year warm events in the historical record are evident in 1957/58, 1962/63, 1991/1992 and 2014/15. Given that the SSTa indices were reconstructed with high skill using local atmospheric forcing, this lead/lag relationship suggests that the atmospheric dynamics, and tropical–subtropical interactions, are an important source of the year-to-year memory, persistence and evolution of the anomaly from the GOA to the ARC pattern.

Large-scale climate mechanisms

Building on previous understanding of the large-scale climate teleconnections of the Pacific Ocean, we use the climate hypothesis of Di Lorenzo *et al.*[23] to examine the dynamics underlying the statistical link between the 2014 and 2015 warm anomalies, and the emergence of multi-year warming events. Inspection of the SSTa for 2014 and 2015 reveals that the anomalies evolved from an NPGO-like pattern in JFM 2014 (Fig. 1a, GOA) to a PDO-like pattern in 2015 (Fig. 1e, ARC), with a weak (∼1 °C) but still significant El Niño expression in the fall of 2014 (Fig. 1c, d black bounding box). This progression of patterns is consistent with the statistical evolution of the SSTa that leads to the ARC pattern (Fig. 3). Previous studies report that the winter JFM 2014 atmospheric forcing pattern is connected to the NPO (for example, the NPGO forcing) and to precursor dynamics of El Niño[2,6,7,24,25]. One of these precursors is linked to the southern lobe of the NPO-like SLPa pattern of 2014 (Fig. 1b), which acts to reduce the speed of the subtropical northeasterly trade winds, which in turn reduce evaporation and increase the local SST. The positive SST anomalies can further reduce the winds and initiate a positive thermodynamic feedback between the ocean and atmosphere known as the winds–evaporation–SST (WES) feedback[26]. This thermodynamic coupled feedback activates

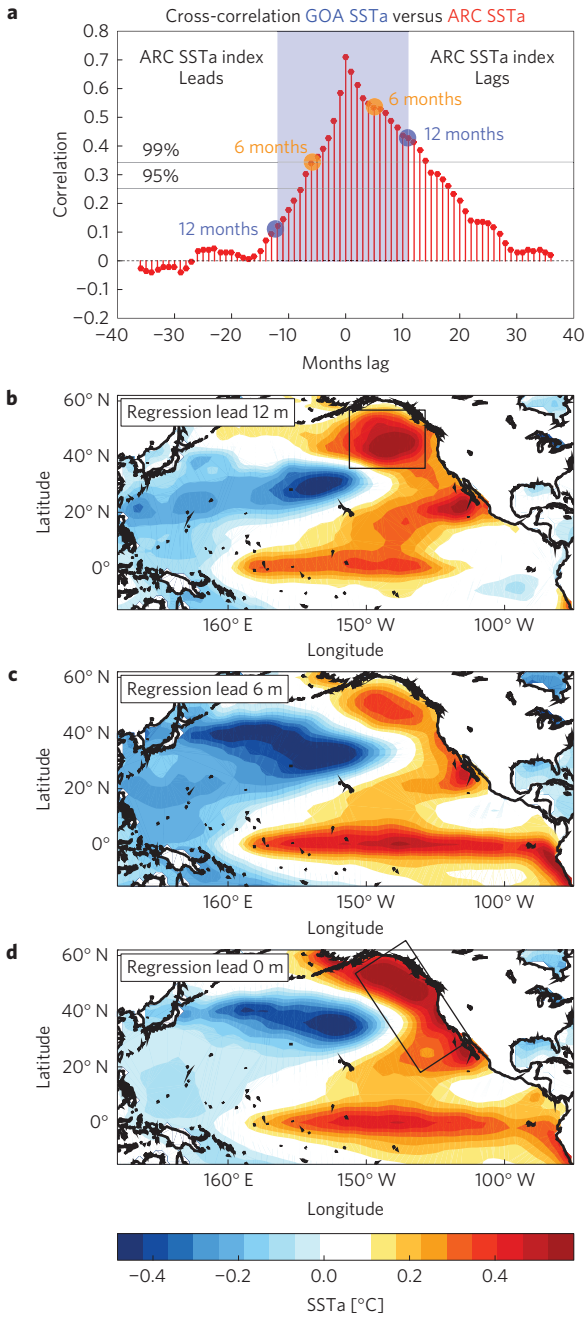

Figure 3 | Lead and lag relationship between SSTa indices for the GOA and ARC patterns. a, Cross-correlation function between the GOA and ARC SSTa indices. **b**–**d**, Regression maps between ARC SSTa indices and SSTa at 0, 6 and 12 month lead showing how the GOA SSTa pattern (**b**) typically evolves into an EL Niño (**c**) followed by the ARC SSTa pattern (**d**). Black boxes define the areas used to define the GOA (**b**) and ARC (**d**) SSTa indices.

the so-called meridional modes[27,28], which propagate and amplify the SSTa from the subtropics into the central equatorial Pacific, where the positive SSTa favour the development of El Niño[24] (Fig. 4, blue path). Once El Niño feedbacks are activated along the Equator, the re-arrangement of tropical convection excites atmospheric Rossby waves in the higher troposphere, which, in the case of an eastern Pacific El Niño, establish atmospheric teleconnections to the extratropics that inject variance onto the Aleutian Low in the next boreal fall/winter season[29]. Changes in the Aleutian Low drive the oceanic expression of the PDO[30,31] (Fig. 4, red path).

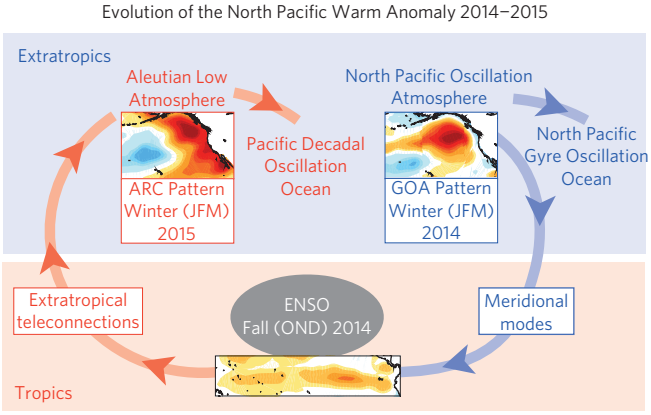

Figure 4 | Climate hypothesis to explain the generation, evolution and persistence of the North Pacific warm anomaly between the winters of 2013/14 and 2014/15.

Although the schematic of Fig. 4 provides a set of deterministic dynamics to explain the statistical link between the North Pacific SSTa of 2014 and 2015, these teleconnection dynamics, and their spatial expressions, are strongly affected by noise in the coupled system. This implies that in any given year the signal associated with the teleconnections may result in a weak or enhanced response of the coupled system. Therefore, it is important to quantify to what extent the tropically forced teleconnections contributed to the strengthening of the North Pacific atmospheric forcing of the JFM 2015 SSTa. We also emphasize that the use of statistical patterns of oceanic and atmospheric variability in the schematic are meant to provide guidance on the nature of the dynamics of the ocean response to atmospheric forcing and of the Pacific climate teleconnections. However, at any given time the coupled system is best represented as a continuum, where the Aleutian Low/PDO and NPO/NPGO represent specific patterns of high interannual and interdecadal variance.

The role of ENSO teleconnections

Over the period of October–November–December (OND) 2014 the tropical Pacific was characterized by SSTa of ∼1 °C with a spatial expression characteristic of El Niño–Southern Oscillation (Fig. 1c). The OND 2014 SLPa also showed a broad area of negative anomalies between Hawaii and western North America that is consistent with a pattern typical of past El Niño events, suggesting that tropical teleconnections may have impacted the SLPa forcing of the SSTa in OND 2014 and JFM 2015.

To quantify what fraction of the northeast Pacific SLPa of OND 2014 and JFM 2015 was forced by teleconnections originating in the tropics, we examine the 50-member ensemble mean SLPa from the International Centre for Theoretical Physics (ICTP) Atmospheric General Circulation Model (AGCM) simulations forced with observed tropical SSTa from 1980–2015 (see Methods). We find that the ensemble average of the SSTa reconstructions inferred from the AGCM output lead to an overall significant skill ($R = 0.56$) in capturing the variability of the ARC SSTa index. According to this simple model reconstruction, tropical teleconnections account for ∼50% (∼1.5 °C) of the peak anomalies of the ARC SSTa index in JFM 2015 (∼3 °C) (Fig. 5a). The 50-member ensemble also includes nine simulations that produce the extreme atmospheric forcing required to account for the observed record-high SSTa in 2015 (Fig. 5b). These results offer strong evidence that tropical forcing contributed significantly in making the JFM 2015 SSTa a record-high event, and in persisting and evolving the extreme northeast Pacific SSTa from 2014 to 2015. Without the contribution from tropical teleconnections, the JFM 2015 SSTa would probably have fallen within the historical range of variability of the northeast

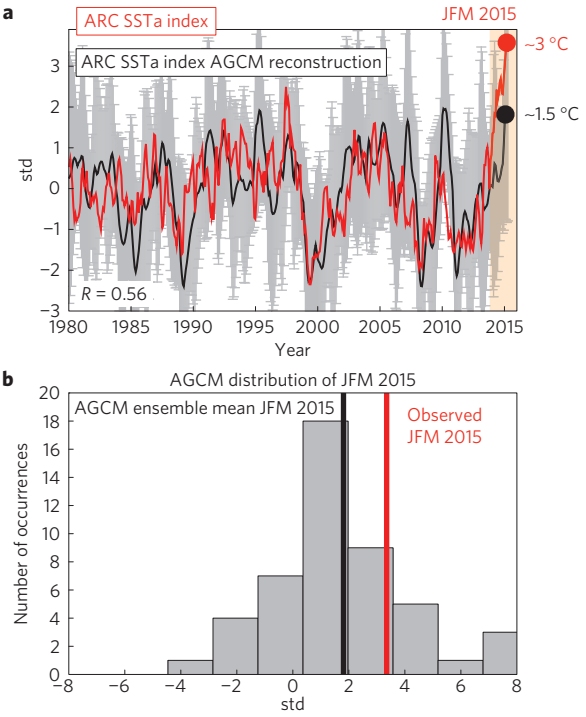

Figure 5 | Fraction of ARC SSTa driven by tropical teleconnections. a, ARC SSTa index (red line) and reconstruction of ARC SSTa (black line) using the tropically forced AGCM simulations (grey bars are 1 standard deviation from the ensemble spread) (see Methods). The time series are in units of standard deviations (std), the size of the anomalies are also reported on the right *y* axis. **b**, Distribution of JFM SSTa for 2015 from the AGCM ensemble members. The AGCM ensemble mean (black line) and the observed (red line) values for JFM 2015 are shown as vertical lines.

Pacific. The skill from the AGCM is consistent with that of a simple observationally based model that uses the OND SSTa in the tropics to predict the following winter JFM SLPa variability in the extratropics ($R = 0.60$, Supplementary Fig. 4).

Climate change implications

The record-breaking character of the 2014–15 marine heatwave raises the question whether these North Pacific Ocean extremes might become more frequent under greenhouse forcing. According to the hypothesis of Fig. 4, the NPO atmospheric forcing, and its ability to excite El Niño teleconnections, is a key player for generating multi-year anomalies in the northeast Pacific. In 2014, the NPO contributed to the extreme drought conditions in California, and previous studies have suggested that this NPO/drought variability, and the El Niño precursor dynamics, will intensify in response to greenhouse forcing[3–5,32].

An intensification of the NPO will carry a strong ocean temperature signature in the variability of the winter (JFM) GOA SSTa pattern (for example, 2014 in Fig. 1a). We test this hypothesis by examining how the winter SSTa variability changes in the 30-member ensemble of the Community Earth System Model Large Ensemble (CESM-LE, see Methods) from 1920–2100 under the RCP8.5 greenhouse scenario. In the CESM-LE and in the observations, the SSTa patterns of the marine heatwave during the winters (JFM) of 2014 and 2015 are captured by the first two empirical orthogonal functions (EOFs) and principal components (PCs) of JFM SSTa over the North Pacific (see Methods, Supplementary Fig. 2). Specifically, PC2/EOF2 tracks the 2014 GOA pattern (for example, NPGO-type), whereas PC1/EOF1 tracks the 2015 ARC pattern (for example, PDO-type). The ensemble means of EOF1 and EOF2 in the CESM-LE map almost exactly onto the EOFs extracted from the NOAA SSTa observational reanalysis ($R > 0.9$, compare Fig. 6 panels a and b versus c and d). The strong similarity between the CESM and the observed EOFs allows us to use the two dominant PCs in the CESM to explore how the winter

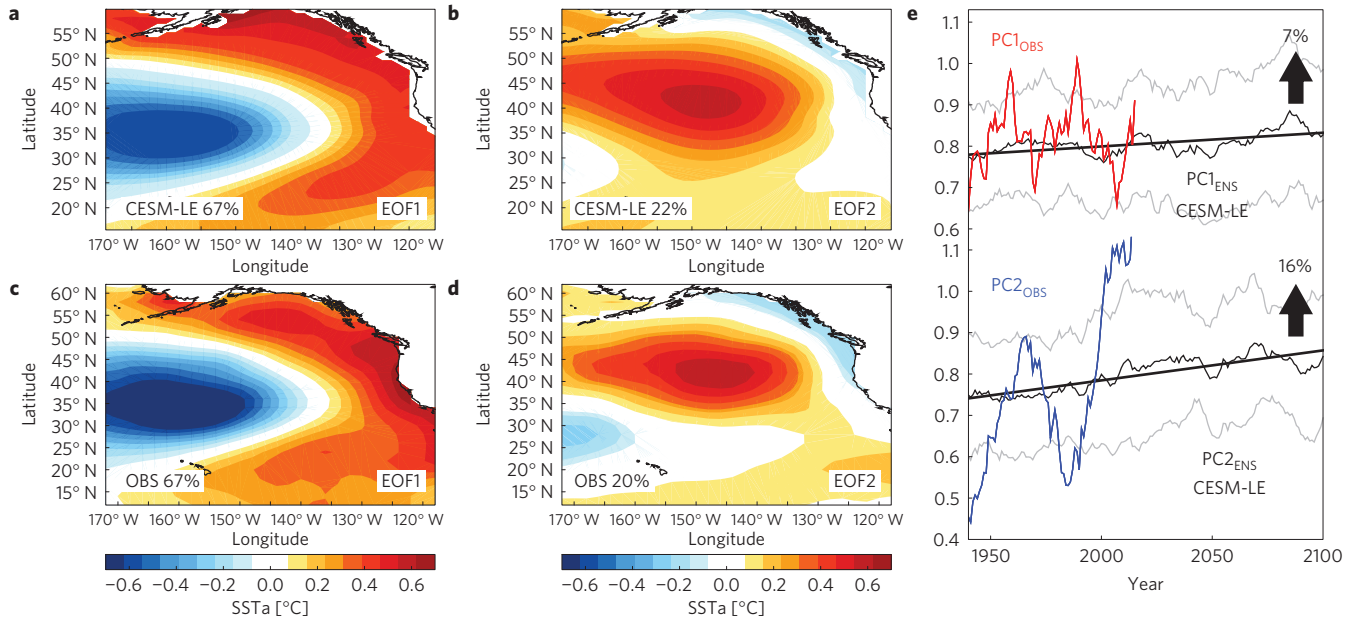

Figure 6 | Changes in the variance of North Pacific climate patterns associated with the northeast Pacific marine heatwaves. a–d, EOF1 (PDO-type, ARC pattern) (**a**,**c**) and EOF2 (NPGO-type, GOA pattern) (**b**,**d**) of JFM SSTa in the CESM-LE (**a**,**b**) and NOAA ERSSTa v3 SSTa (**c**,**d**). For the CESM-LE, EOFs are computed for each of the 30 simulations and the ensemble mean is presented. The amount of variance explained by each mode is reported in the bottom of the panels. **e**, Running standard deviation calculated over 20 years for the PC1 and PC2 of each ensemble member. The black line represents the ensemble mean, while the grey lines mark the one standard deviation of the ensemble spread. The same analysis is done for the one realization of the observed PC1 and PC2 of JFM SSTa. Before analyses of the CESM-LE data, a quadratic trend has been removed at each grid point of the SSTa for each of the 30 simulations to avoid artificial changes in variance associated with the trend.

patterns associated with the 2014/15 marine heatwave are expected to change in the future. According to the CESM-LE, the variances of PC1 and PC2 increase significantly under greenhouse forcing, by ~7% and ~16% (Fig. 6e), suggesting that the PDO- and NPGO-type variance is increasing in a warmer climate. Unfortunately, the single observational records available for the PC1 (for example, SSTa ARC JFM index) and PC2 (for example, SSTa GOA JFM index) are too short to attribute observational significance to this finding (Fig. 6e). Other studies[33] that evaluated the statistics of simulated GOA SST from CMIP5 pre-industrial control and historical forcing experiments also found that anthropogenic forcing has increased the risk for observing regional SSTa extremes similar to those of 2014 by a factor of five over natural variability alone.

To date, no clear mechanism has been identified to explain the projected intensification of the NPO/NPGO-type activity. Given that the NPO is linked to the activity of meridional modes and their thermodynamic coupling between ocean and atmosphere, it is possible that, as the mean surface temperatures of the tropical and subtropical Pacific continue to rise, the thermodynamic feedbacks (for example, WES) may intensify. This would lead to enhanced variance of the NPO system, leading to stronger atmospheric and SST anomalies in the extratropics, and stronger SSTa in the tropics. The stronger SSTa in the tropics could account for an intensification of the El Niño response to the NPO, leading to an enhanced coupling between tropics and extratropics, and between the NPGO-like and PDO-like variability. Testing mechanistic hypothesis such as these in models of ranging complexity may allow for more robust estimates of how the statistics of ocean extremes in the northeast Pacific are influenced by greenhouse forcing.

Methods

Methods and any associated references are available in the online version of the paper.

Received 22 March 2016; accepted 1 June 2016;
published online 11 July 2016

References

1. Bond, N. A., Cronin, M. F., Freeland, H. & Mantua, N. Causes and impacts of the 2014 warm anomaly in the NE Pacific. *Geophys. Res. Lett.* **42,** 3414–3420 (2015).
2. Baxter, S. & Nigam, S. Key role of the North Pacific oscillation-West Pacific pattern in generating the extreme 2013/14 North American winter. *J. Clim.* **28,** 8109–8117 (2015).
3. Wang, S. Y., Hipps, L., Gillies, R. R. & Yoon, J. H. Probable causes of the abnormal ridge accompanying the 2013–2014 California drought: ENSO precursor and anthropogenic warming footprint. *Geophys. Res. Lett.* **41,** 3220–3226 (2014).
4. Wang, S. Y. S., Huang, W. R. & Yoon, J. H. The North American winter 'dipole' and extremes activity: a CMIP5 assessment. *Atmos. Sci. Lett.* **16,** 338–345 (2015).
5. Yoon, J. H. *et al*. Increasing water cycle extremes in California in relation to ENSO cycle under global warming. *Nature Commun.* **6,** 6 (2015).
6. Vimont, D. J., Wallace, J. M. & Battisti, D. S. The seasonal footprinting mechanism in the Pacific: implications for ENSO. *J. Clim.* **16,** 2668–2675 (2003).
7. Anderson, B. T. Tropical Pacific sea-surface temperatures and preceding sea level pressure anomalies in the subtropical North Pacific. *J. Geophys. Res.* **108,** 4732 (2003).
8. Hobday, A. J. *et al*. A hierarchical approach to defining marine heatwaves. *Prog. Oceanogr.* **141,** 227–238 (2016).
9. Whitney, F. A. Anomalous winter winds decrease 2014 transition zone productivity in the NE Pacific. *Geophys. Res. Lett.* **42,** 428–431 (2015).
10. Peterson, W., Bond, N. & Robert, M. The Blob (Part Three): Going, going, gone? *PICES Press* **24,** 46–48 (2016).
11. Opar, A. Lost at sea: starving birds in a warming world. *Audubon Magazine* (2015); https://www.audubon.org/magazine/march-april-2015/lost-sea-starving-birds-warming-world
12. *2015 Large whale Unusual Mortality Event in the Western Gulf of Alaska* (NOAA, 2016); http://www.nmfs.noaa.gov/pr/health/mmume/large_whales_2015.html
13. *2013–2016 California Sea Lion Unusual Mortality Event in California* (NOAA, 2016); http://www.nmfs.noaa.gov/pr/health/mmume/californiasealions2013.htm
14. *NOAA Fisheries Mobilizes to Gauge Unprecedented West Coast Toxic Algal Bloom* (NOAA, 2016); http://www.nwfsc.noaa.gov/news/features/west_coast_algal_bloom/index.cfm
15. Hartmann, D. L. Pacific sea surface temperature and the winter of 2014. *Geophys. Res. Lett.* **42,** 1894–1902 (2015).
16. Seager, R. *et al*. Causes of the 2011–14 California Drought. *J. Clim.* **28,** 6997–7024 (2015).
17. Anderson, B. T., Gianotti, D. J. S., Furtado, J. C. & Di Lorenzo, E. A decadal precession of atmospheric pressures over the North Pacific. *Geophys. Res. Lett.* **43,** 3921–3927 (2016).
18. Di Lorenzo, E. *et al*. North Pacific Gyre Oscillation links ocean climate and ecosystem change. *Geophys. Res. Lett.* **35,** L08607 (2008).
19. Bond, N. A., Overland, J. E., Spillane, M. & Stabeno, P. Recent shifts in the state of the North Pacific. *Geophys. Res. Lett.* **30,** 2183 (2003).
20. Mantua, N. J., Hare, S. R., Zhang, Y., Wallace, J. M. & Francis, R. C. A Pacific interdecadal climate oscillation with impacts on salmon production. *Bull. Am. Meteorol. Soc.* **78,** 1069–1079 (1997).
21. Chhak, K. C., Di Lorenzo, E., Schneider, N. & Cummins, P. F. Forcing of low-frequency ocean variability in the Northeast Pacific. *J. Clim.* **22,** 1255–1276 (2009).
22. Johnstone, J. A. & Mantua, N. J. Atmospheric controls on northeast Pacific temperature trends and variations, 1900–2012. *Proc. Natl Acad. Sci.* **111,** 14360–14365 (2014).
23. Di Lorenzo, E. *et al*. ENSO and meridional modes: a null hypothesis for Pacific climate variability. *Geophys. Res. Lett.* **42,** 9440–9448 (2015).
24. Alexander, M. A., Vimont, D. J., Chang, P. & Scott, J. D. The Impact of extratropical atmospheric variability on ENSO: testing the seasonal footprinting mechanism using coupled model experiments. *J. Clim.* **23,** 2885–2901 (2010).
25. Anderson, B. T., Perez, R. C. & Karspeck, A. Triggering of El Niño onset through the trade-wind induced charging of the equatorial Pacific. *Geophys. Res. Lett.* **40,** 1212–1216 (2013).
26. Xie, S. P. A dynamic ocean–atmosphere model of the tropical Atlantic decadal variability. *J. Clim.* **12,** 64–70 (1999).
27. Chiang, J. C. H. & Vimont, D. J. Analogous Pacific and Atlantic meridional modes of tropical atmosphere-ocean variability. *J. Clim.* **17,** 4143–4158 (2004).
28. Vimont, D. J. Transient growth of thermodynamically coupled variations in the tropics under an equatorially symmetric mean. *J. Clim.* **23,** 5771–5789 (2010).
29. Alexander, M. A. *et al*. The atmospheric bridge: the influence of ENSO teleconnections on air–sea interaction over the global oceans. *J. Clim.* **15,** 2205–2231 (2002).
30. Newman, M., Compo, G. P. & Alexander, M. A. ENSO-forced variability of the Pacific Decadal Oscillation. *J. Clim.* **16,** 3853–3857 (2003).
31. Schneider, N. & Cornuelle, B. D. The forcing of the Pacific Decadal Oscillation. *J. Clim.* **18,** 4355–4373 (2005).
32. Sydeman, W. J., Santora, J. A., Thompson, S. A., Marinovic, B. & Di Lorenzo, E. Increasing variance in North Pacific climate relates to unprecedented ecosystem variability off California. *Glob. Change Biol.* **19,** 1662–1675 (2013).
33. Weller, E. *et al*. Human contribution to the 2014 record high sea surface temperatures over the western tropical and northeast Pacific Ocean [in "Explaining Extremes of 2014 from a Climate Perspective"]. *Bull. Am. Meteorol. Soc.* **96,** S100–S104 (2015).

Acknowledgements

We acknowledge the support of the NSF-OCE 1356924, NSF-OCE 1419292 and NSF CCE-LTER. We also thank N. Schneider for feedback and discussion provided.

Author contributions

E.D.L. and N.M. envisioned and wrote the paper. E.D.L. designed and executed the analyses.

Additional information

Supplementary information is available in the online version of the paper. Reprints and permissions information is available online at www.nature.com/reprints. Correspondence and requests for materials should be addressed to E.D.L.

Competing financial interests

The authors declare no competing financial interests.

Methods

Sea surface temperature (SST) and sea-level pressure (SLP) datasets. To reconstruct the ocean and atmospheric variability associated with the northeast Pacific warm anomalies we use the National Oceanic and Atmospheric Administration (NOAA) Extended Reconstruction SST, version 3 (ERSST.v3) product[34]. The data are available on a 2° × 2° horizontal grid globally for the period 1880 to the present. Monthly mean SLP data and anomalies are taken from the National Centers for Environmental Prediction-National Center for Atmospheric Research reanalysis product[35] and exist on a 2.5° × 2.5° horizontal grid globally. We analyse the data over the period to 1980–2015. Anomalies for both SST and SLP are constructed by removing the mean monthly climatology computed over the period 1980–2015. A linear trend is removed from the SST and SLP anomalies at each grid point.

Definition of oceanic SSTa indices. The strength of the 2014 and 2015 anomaly patterns is measured by taking the average SSTa in the regions centred around the peak anomalies in the GOA region (Fig. 1a, blue box for 2014 pattern) and along the Pacific North American boundary, also referred to as the 'ARC' (Fig. 1e, red box for the 2015 pattern). We refer to these indices as the GOA SSTa index (Fig. 2c) and the ARC SSTa index (Fig. 2d), respectively. The winter average January–February–March (JFM) values of these indices are also reported for the entire ERSST.v3 period 1880–2015 in Supplementary Fig. 1.

Definition of atmospheric SLPa indices. To construct indices of the atmospheric forcing functions of the marine heatwave, we project the full SLPa field, $\mathrm{SLPa}\,(x,y,t)$, on the SLPa patterns for JFM 2014 and JFM 2015, respectively, over the forcing region of the central and eastern North Pacific [180° W 100° W; 10° N 62° N] (Fig. 1b and f, black boxes).

$$\text{SLPa Index}_{\text{GOA}}\,(t) = \int\int \text{SLPa}_{\text{JFM2014}}\,(x,y)\;\text{SLPa}(x,y,t)\mathrm{d}x\mathrm{d}y \tag{1}$$

$$\text{SLPa Index}_{\text{ARC}}\,(t) = \int\int \text{SLPa}_{\text{JFM2015}}\,(x,y)\;\text{SLPa}(x,y,t)\mathrm{d}x\mathrm{d}y \tag{2}$$

This procedure allows us to generate historical time series for the strength of the atmospheric forcing patterns that were important in driving the 2014 and the 2015 SSTa patterns, respectively (Fig. 2a,b).

Auto-regressive model to reconstruct SSTa. We reconstruct the GOA and ARC SSTa indices using a simple 1D auto-regressive model forced by the corresponding SLPa indices,

$$\frac{\text{dSSTa Index}\,(t)}{\mathrm{d}t} = \alpha\,\text{SLPa Index}\,(t) - \frac{\text{dSSTa Index}\,(t)}{\tau} \tag{3}$$

where α is a scaling factor associated with the forcing term and τ is a damping timescale associated with the dissipation term. This simple 1D auto-regressive model of order 1 (AR-1) has been widely used to reconstruct ocean response to atmospheric forcing in the North Pacific[21,31], and is consistent with previous findings documenting how northeast Pacific SSTa variability over 1900 to 2012 was driven by atmospheric forcing that alters surface heat flux, Ekman transport, and entrainment into the ocean mixed layer[22]. Following these previous studies, we estimate the damping timescale for the SSTa indices from the e-folding timescale of their auto-correlation function $\tau = 8$ months. Before running the model, we normalize the SLPa indices by their standard deviations and set the scaling factor $\alpha = 1$. This leads to SSTa reconstructions in units of standard deviations.

AGCM ensemble modelling. To diagnose the role of tropically generated atmospheric teleconnections in forcing atmospheric anomalies over the region of the northeast Pacific anomaly, we use an ensemble of coupled ocean–atmosphere modelling experiments conducted with the International Center for Theoretical Physics (ICTP) Atmosphere General Circulation Model (AGCM) coupled to a 50 m slab ocean. This AGCM, also known as SPEEDY, uses eight vertical layers and T30 horizontal resolution. Climatological heat fluxes corrected through observations are prescribed to account for ocean heat transport. The physical parameterizations of the model are described by Molteni[36], and prior applications of this configuration can be found in Bracco *et al.*[37]. To reconstruct the fraction of North Pacific atmospheric variability forced by the tropics we prescribed de-trended SSTa from 1980 to 2015 in a narrow region along the entire tropical belt (12° S–12° N) as a surface boundary condition to drive a 50-member ensemble of the ICTP AGCM with the slab ocean. Away from this tropical region, interactive fluxes between the AGCM and the slab ocean are implemented to determine the SSTa field. By examining the ensemble mean SLPa from the 50 members, we effectively remove all contributions of stochastic forcing from the North Pacific SLPa and identify the SLPa variance that is driven by tropical forcing. This approach and model have been used in previous studies that diagnose the role of El Niño teleconnections in the extratropics[38].

The ensemble mean of SLPa over the North Pacific effectively removes all contributions of extratropical stochastic forcing and retains only the portion of North Pacific SLPa variability that is driven by tropical atmospheric teleconnections forced by the tropical SSTa boundary conditions. The spread in the ensemble provides a measure for the combined influences of stochastic forcing and the tropical-origin forced teleconnections. Using the same approach as described for the observational analyses, we reconstruct the North Pacific SLPa forcing index by projecting the AGCM SLPa field, $\widehat{\text{SLPa}}_{\text{AGCM}}(x,y,t)$, onto the OND 2014 SLPa pattern of the North Pacific in the region (180°–100° W; 10°–62° N) (black box in Fig. 1f). We use the OND 2014 pattern, $\widehat{\text{SLPa}}_{\text{OND2014\_AGCM}}(x,y)$, to capture the variability associated with the fall SSTa-forced teleconnections in the AGCM because OND is the time when the El Niño-like SSTa is strongest in the tropics (black boxes in Fig. 1c,d).

$$\widehat{\text{SLPa}}\ \text{Index}_{\text{CCS}}\,(t) = \int\int \widehat{\text{SLPa}}_{\text{OND2014\_AGCM}}(x,y)\widehat{\text{SLPa}}_{\text{AGCM}}(x,y,t)\mathrm{d}x\mathrm{d}y \tag{4}$$

The $\widehat{\text{SLPa}}\ \text{Index}_{\text{CCS}}\,(t)$ captures the fraction of tropically forced variability of the atmospheric pattern responsible for the winter 2014/15 SSTa along the North American coastal boundary. We now use the AGCM-derived atmospheric forcing index from each ensemble member to force the AR-1 model (equation (3)) and reconstruct the time variability of the ARC SSTa index (Fig. 5).

CESM-LE ensemble data archive. We use output of the first 30 members of the Community Earth System Model (CESM) Large Ensemble simulations from 1920–2100 under the RCP8.5 greenhouse scenario available at https://www2.cesm.ucar.edu/models/experiments/LENS[39]. The 30-member ensemble uses historical radiative forcing for the period 1920–2005 and RCP8.5 radiative forcing thereafter. The simulation uses a 1-degree latitude/longitude version of CESM1(CAM5).

Empirical orthogonal functions (EOFs) of winter SSTa. The first two EOFs and principal components (PCs) of winter (JFM) SSTa over the northeast Pacific (180° W–110° W; 10° N–62° N) are computed for the CESM-LE over the period 1920–2100 and for the ERSST.v3 reanalysis over the period 1920–2015. Before the computation of the EOFs, a linear and quadratic trend is removed at each grid point from the SSTa data. In the CESM-LE, the EOFs and PCs are computed for each of the 30 ensemble members. The ensemble average of the EOF1 and EOF2 spatial patterns are then computed (Fig. 6a,b). After computation of the EOFs we further verify that no significant trends exist in the PCs. The same EOFs approach is used on the available observations (Fig. 6c,d). The correlation between the observed (ERSST.v3) and modelled (CESM-LE) spatial patterns of EOF1 and EOF2 is highly significant ($R = 0.94$ and $R = 0.92$). Given that the observed PC2/EOF2 and PC1/EOF1 closely track the GOA and ARC patterns (Supplementary Fig. 2), we use the CESM-LE EOFs and PCs to characterize the changes in variance of the northeast Pacific marine heatwave patterns under greenhouse forcing.

References

34. Smith, T. M., Reynolds, R. W., Peterson, T. C. & Lawrimore, J. Improvements to NOAA's historical merged land–ocean surface temperature analysis (1880–2006). *J. Clim.* **21,** 2283–2296 (2008).
35. Kalnay *et al*. The NCEP/NCAR 40-year reanalysis project. *Bull. Am. Meteorol. Soc.* **77,** 437–470 (1996).
36. Molteni, F. Atmospheric simulations using a GCM with simplified physical parametrizations. I: model climatology and variability in multi-decadal experiments. *Clim. Dynam.* **20,** 175–191 (2003).
37. Bracco, A., Kucharski, F., Kallummal, R. & Molteni, F. Internal variability, external forcing and climate trends in multi-decadal AGCM ensembles. *Clim. Dynam.* **23,** 659–678 (2004).
38. Di Lorenzo, E. *et al*. Central Pacific El Nino and decadal climate change in the North Pacific Ocean. *Nature Geosci.* **3,** 762–765 (2010).
39. Kay, J. E. *et al*. The Community Earth System Model (CESM) large ensemble project: a community resource for studying climate change in the presence of internal climate variability. *Bull. Am. Meteorol. Soc.* **96,** 1333–1349 (2015).